Single amino acid substitution in *Plasmodium yoelii* erythrocyte ligand determines its localization and controls parasite virulence

Hitoshi Otsuki[a], Osamu Kaneko[a,b,1], Amporn Thongkukiatkul[a,c], Mayumi Tachibana[a], Hideyuki Iriko[a,d], Satoru Takeo[e], Takafumi Tsuboi[e], and Motomi Torii[a]

[a]Department of Molecular Parasitology, Ehime University Graduate School of Medicine, Toon, Ehime 791-0295, Japan; [b]Department of Protozoology, Institute of Tropical Medicine (NEKKEN) and the Global Center of Excellence Program, Nagasaki University, Nagasaki, Nagasaki 852-8523, Japan; [c]Department of Biology, Burapha University, Amphur Muang, Chonburi 20131, Thailand; [d]Department of Microbiology and Pathology, Faculty of Medicine, Tottori University, Yonago, Tottori 683-8503, Japan; and [e]Cell-Free Science and Technology Research Center, Ehime University, Matsuyama, Ehime 790-8577, Japan

The major virulence determinant of the rodent malaria parasite, *Plasmodium yoelii*, has remained unresolved since the discovery of the lethal line in the 1970s. Because virulence in this parasite correlates with the ability to invade different types of erythrocytes, we evaluated the potential role of the parasite erythrocyte binding ligand, *Py*EBL. We found 1 amino acid substitution in a domain responsible for intracellular trafficking between the lethal and nonlethal parasite lines and, furthermore, that the intracellular localization of *Py*EBL was distinct between these lines. Genetic modification showed that this substitution was responsible not only for *Py*EBL localization but also the erythrocyte-type invasion preference of the parasite and subsequently its virulence in mice. This previously unrecognized mechanism for altering an invasion phenotype indicates that subtle alterations of a malaria parasite ligand can dramatically affect host–pathogen interactions and malaria virulence.

dense granule | invasion | malaria | microneme | transfection

The rodent malaria parasite *Plasmodium yoelii yoelii* has been widely studied to understand the interactions between the malaria parasite and the host cell (1). The nonlethal 17X line mainly infects young erythrocytes (reticulocytes), whereas the lethal 17XL and YM lines infect a wide range of erythrocytes. These lines have previously been studied to identify the genetic determinants of virulence (2, 3). These differences in erythrocyte invasion preference suggest the possible involvement of a parasite ligand that recognizes erythrocyte surface receptors; however, the actual molecular basis of the observed invasion preference differences remains unclear.

Erythrocyte invasion by the malaria merozoite is a multistep process, initiated by reversible binding to the erythrocyte surface, followed by the establishment of a tight junction between the apical end of the merozoite and erythrocyte surface and the subsequent movement of the merozoite into the nascent parasitophorous vacuole. Each step involves specific interactions between parasite ligands and erythrocyte receptors. Among the ligands of malaria parasites, the best characterized is a type I integral transmembrane protein encoded by the *ebl* (*erythrocyte-binding-like*) gene family. Upon release from the micronemes, EBL proteins recognize erythrocyte receptors and initiate the formation of the tight junction. The importance of EBL in malaria virulence is exemplified in the human malaria parasite *Plasmodium vivax*, which uses an EBL orthologue, *Pv*DBP, to recognize the Duffy antigen on the erythrocyte surface. Because the parasite is apparently unable to use an alternative invasion pathway, individuals in whom the Duffy antigen is not expressed on the erythrocyte surface are completely resistant to *P. vivax* (4, 5). Because of this dramatic association between the disruption of a host–pathogen interaction and protection against a malaria

parasite, *Pv*DBP and the *Plasmodium falciparum* EBL orthologue, EBA-175, have been targeted for vaccine development (6).

EBL proteins possess 2 Cys-rich regions conserved among EBL orthologues. The N-terminal Cys-rich region named the DBL (Duffy-binding-like) domain or region 2 (7) recognizes a specific erythrocyte surface receptor. The C-terminal Cys-rich region named the C-cys domain or region 6 is located adjacent to the transmembrane domain, and the number and location of Cys residues are well conserved among known *Plasmodium* species. Region 6 exhibits structural similarity to the KIX-binding domain of the coactivator CREB-binding protein (8) and has been proposed to be a protein trafficking signal for transportation to the micronemes (9). Here we report a single nonsynonymous nucleotide substitution in the *pyebl* gene between lethal and nonlethal lines of *P. yoelii* and show the effect of this substitution on the intracellular localization of EBL, erythrocyte-type preference, and consequently virulence of *P. yoelii*.

Results

To investigate differences in EBL between lethal and nonlethal *P. yoelii* lines, we compared sequences from a variety of malaria parasite species and *P. yoelii* lines 17X, 17XL, and YM. We found 1 nonsynonymous nucleotide substitution in region 6 between the nonlethal 17X and lethal 17XL lines in the entire ORF (Fig. 1). The nonlethal 17X line possesses 8 conserved Cys residues that form 4 disulfide bridges (8), whereas the lethal 17XL line possesses an Arg instead of Cys at the second Cys position. This substitution was also found in another lethal line, "YM" (2), which originated independently from the 17X line during serial passage (3). All *Plasmodium* EBL orthologues for which protein expression was validated possess 8 conserved Cys residues in this region, further indicating that these Cys residues play an important role (supporting information Fig. S1). Thus the observed substitution from Cys to Arg is likely to abolish the native conformation of region 6.

EBL Localizes in the Dense Granules in *P. yoelii* Line 17XL. We raised specific polyclonal and monoclonal antibodies against *Py*EBL

MICROBIOLOGY
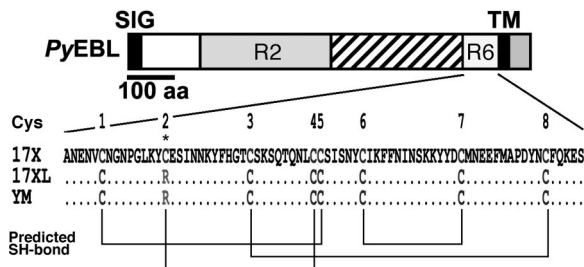
Fig. 1. Schematic structure of *P. yoelii* EBL (*Py*EBL). SIG, TM, R2, and R6 indicate the putative endoplasmic reticulum transporting signal, the transmembrane region, region 2, and region 6, respectively. Amino acid alignment of *Py*EBL from 17X, 17XL, and YM lines are shown below. Eight conserved Cys residues that form disulfide bridges (Predicted SH-bond) and the substitution from Cys to Arg (*) are indicated.

and performed Western blot analysis. The *Py*EBL protein was detected as a 110-kDa band in both the 17X and 17XL lines (Fig. 2*A*). The intracellular localization of *Py*EBL in both the 17X and 17XL lines was compared by indirect immunofluorescent assay
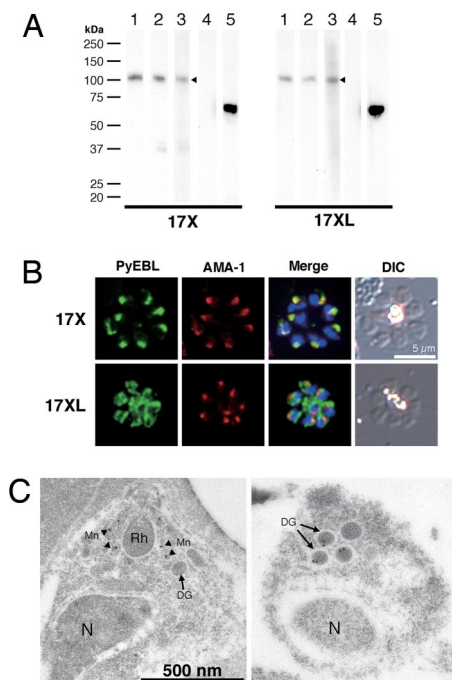
Fig. 2. Western blot analysis and *Py*EBL localization in *P. yoelii* schizont by immunostaining. (*A*) Western blot analysis with mAb 5B10 (lane 1), mAb 1G10 (lanes 2), and mouse serum (lane 3) specific for *Py*EBL against purified *P. yoelii* schizont extracts. A 110-kDa band was detected in both 17X and 17XL lines, with no significant difference in the protein expression level (arrowheads). This band was not detected by normal mouse serum (lane 4). Anti-AMA1 serum detected a 66-kDa band at similar levels (lane 5). (*B*) *P. yoelii* schizonts were incubated with mAb 5B10 (*Py*EBL), rabbit anti-AMA1 serum (AMA1), and DAPI (blue) for nuclear staining. Schizonts labeled with anti-*Py*EBL (5B10) were stained with FITC secondary antibody (green). Anti-AMA1 were stained with Alexa-546 secondary antibody (red). DIC images are shown in the right-hand column. The 17X line shows apical *Py*EBL signal colocalized with AMA1, but the region 6–substituted 17XL line shows diffused staining that does not colocalize with AMA1. (*C*) Immunoelectron micropcopy was carried out for resin-embedded *P. yoelii* 17X and 17XL lines with anti-*Py*EBL mouse serum and secondary antibody conjugated with gold particles. *Py*EBL was detected in the micronemes (arrowheads) of the 17X line, but in the 17XL line it was located in the dense granules (arrows). N, nucleus; Mn, microneme; DG, dense granule; Rh, rhoptry.
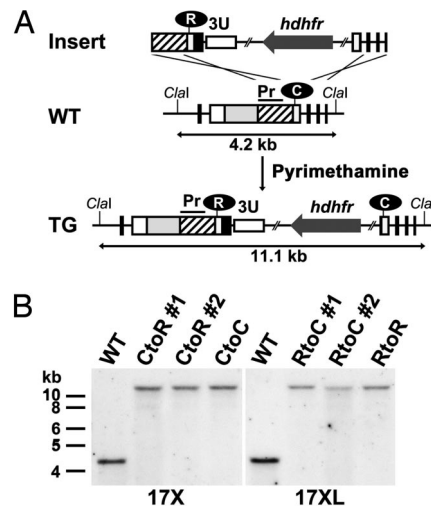

Fig. 3. Amino acid replacement of *Py*EBL region 6 second cysteine location by targeted recombination. (*A*) Schematic representation of the WT and modified (TG) *pyebl* gene loci. The replacement cassette (Insert) was inserted into the *pyebl* gene locus by double-crossover recombination. In this schematic, the second Cys in region 6 was replaced with Arg in the 17X line to generate 17X-CtoR. Other transgenic lines were generated in a similar fashion. ClaI restriction sites and the expected size of the DNA fragment after ClaI digestion are shown. Pr, probe region used in Southern blot analysis. (*B*) Southern blot analysis of the *pyebl* gene locus in WT and transgenic parasite lines derived from *P. yoelii* 17X and 17XL. The absence of the 4.2-kb WT band and the presence of an 11.1-kb band indicate that the *Py*EBL locus was modified in all transgenic clones.

(IFA) using specific antibodies against *Py*EBL (Fig. S2). In the 17X line, *Py*EBL localized to the apical end of each merozoite in both the segmented schizont-stage parasite and individual merozoites, where it colocalized with AMA1, a known microneme protein, under immunofluorescent microscopy (Fig. 2*B*). However, in the 17XL line *Py*EBL did not colocalize with AMA1 at the apical end of merozoites and showed a more diffused but granular distribution in comparison with parasites of the 17X line (Fig. 2*B*). Diffused localization of *Py*EBL was also observed in parasites of the YM line (Fig. S3). Immunoelectron microscopy revealed that *Py*EBL localized in micronemes in the 17X line as reported for *P. falciparum* and *Plasmodium knowlesi* (10, 11). In the 17XL line, however, *Py*EBL localized not in the microneme but in another microorganelle—the dense granules (12) (Fig. 2*C* and Fig. S4).

Because there seems to be only 1 copy of *Py*EBL in the genomes of both lines (Fig. S5), and significant differences were not observed in the level of transcription and protein expression between the 17X and 17XL lines (Fig. 2*A* and Fig. S6), the location of EBL seems to be the most significant difference between them.

Genetic Replacement of Arg and Cys in Region 6 Alters EBL Localization. To evaluate whether the Arg substitution at the second Cys position is responsible for the altered trafficking of *Py*EBL, we exchanged Cys and Arg in the 17X and 17XL lines by genetic modification (17X-CtoR and 17XL-RtoC). The parasites were also transfected with control constructs that do not alter the region 6 amino acid sequence (17X-CtoC and 17XL-RtoR) (Fig. 3*A*). Each of the transgenic parasites was evaluated for the correct integration of the constructs to the *pyebl* gene locus by specific PCR analysis followed by sequencing of the PCR-amplified products (not shown) and Southern blot analysis (Fig. 3*B*).

In the 17X line, replacement of Cys with Arg (17X-CtoR) altered the *Py*EBL localization from an apical pattern to a
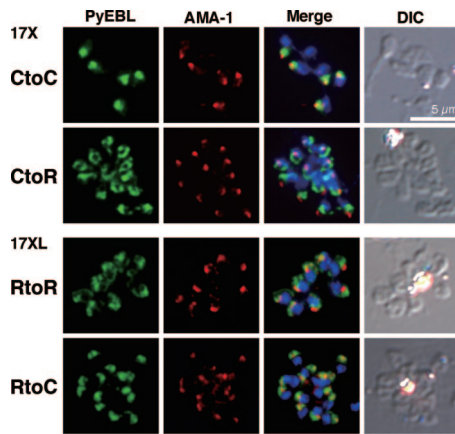
Fig. 4. Replacement of Cys to Arg in region 6 altered subcellular localization of *Py*EBL. Schizonts of transgenic parasite lines were incubated with mAb 5B10 (*Py*EBL), rabbit anti-AMA1 serum (AMA1), and DAPI (blue) for nuclear staining. DIC images are shown in the right-hand column. In the 17X background, control (CtoC) shows an apical *Py*EBL signal colocalized with AMA1, but replaced (CtoR) shows a 17XL pattern. Inversely, 17XL background control (RtoR) shows a diffused nonapical pattern, but replaced to cysteine (RtoC) shows an apical signal colocalized with AMA1.

nonapical diffused pattern, and *Py*EBL did not colocalize with AMA1. Furthermore, the replacement of Arg with Cys in the 17XL line (17XL-RtoC) altered the *Py*EBL localization from a nonapical diffused pattern to an apical pattern. Control parasites did not display altered *Py*EBL localization (Fig. 4). These results confirm that the observed substitution from Cys to Arg is responsible for the altered localization of *Py*EBL from micronemes to dense granules in the 17XL line.

EBL Localization Alters Erythrocyte-Type Preference and Course of Infection. To determine whether altered localization of *Py*EBL affects erythrocyte-type invasion preference, infected erythrocytes were examined by microscopy, and a selectivity index (SI) was obtained by calculating multiple parasite infection of single erythrocytes for each parasite line on postinfection day 3 in mice (13). We found that 17XL-RtoC predominantly invaded reticulocytes in the same way as the nonlethal 17X line. The SI of the 17XL line (2.38) was increased in 17XL-RtoC ($\approx$35; $P < 0.001$). On the other hand, 17X-CtoR was able to invade a variety of ages of erythrocytes, including mature erythrocytes, comparable to the lethal 17XL line, with the SI of the 17X line (16.78) reduced in 17X-CtoR ($\approx$4; $P < 0.001$; Table 1). These results demon-

Table 1. Selectivity index of WT and transgenic *Plasmodium yoelii* lines

| Parasite	*n*	Selectivity index (range)
17X-CtoR 1	5	3.87 (1.86–5.32)
17X-CtoR 2	5	4.25 (2.38–7.97)
17X-CtoC	5	23.53 (16.49–36.00)
17X	5	16.78 (7.60–24.99)
17XL-RtoC 1	5	34.35 (29.18–38.05)
17XL-RtoC 2	5	35.99 (29.97–42.72)
17XL-RtoR	5	1.31 (0.57–2.13)
17XL	5	2.38 (1.58–3.75)

Selectivity indices were calculated from parasitized Giemsa-stained thin blood films collected from each infection.

strate that the localization of *Py*EBL is responsible for the erythrocyte-type preference of the parasite.

Because erythrocyte-type preference frequently correlates with virulence in malaria parasites, we further analyzed the transgenic *P. yoelii* parasites for differences in the course of infection and survival of parasite-infected mice. Mice infected with the 17XL-RtoC line developed significantly lower parasitemias compared with the parental 17XL and control 17XL-RtoR lines (Fig. 5A), with 100% survival (Fig. 5C), whereas all mice infected with 17XL and 17XL-RtoR lines died by day 7 (Fig. 5C). The pattern observed for the 17XL-RtoC line was identical to that observed for the nonlethal 17X line. Thus, trafficking of *Py*EBL to the micronemes causes the virulence of the 17XL line to be reduced to the same level as the nonlethal 17X line, suggesting that *Py*EBL is a critical virulence determinant in the 17XL line. The parasitemia of mice infected with 17X-CtoR increased significantly compared with those infected with parental 17X and control 17X-CtoC lines during the acute phase of infection on days 4 to 5 ($P < 0.001$). However, the parasitemia did not reach the level observed for the lethal 17XL line, and it reduced to the same level observed for the 17X and 17X-CtoC lines by day 9 (Fig. 5B). No parasites were detectable by microscopy at day 17 (not shown). This suggests that the 17X-CtoR line is able to invade a greater repertoire of erythrocyte types than 17X but is unable to invade as many types as the 17XL line. This reduced capacity to invade multiple erythrocyte types compared with the 17XL line results in a nonlethal infection, in which all mice survive (Fig. 5C). Thus, displacement of the EBL from microneme was not sufficient to make this line fully lethal, suggesting the existence of other determinant(s).

Discussion

The results of this study indicate that replacement of Cys to Arg at the second Cys position of *Py*EBL region 6 is the major
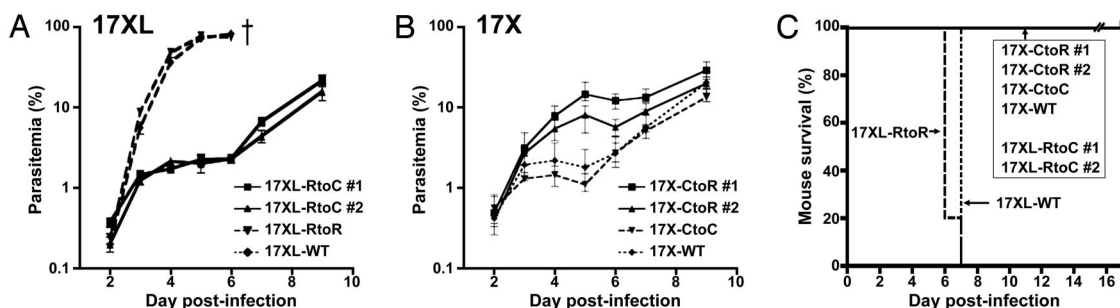
Fig. 5. Effect of the alteration of *pyebl* gene loci on the course of infection and parasite virulence in mice. Mice were i.v. inoculated with 1×10^6 parasitized erythrocytes from WT or transgenic parasite lines. (A) Parasitemia of 17XL-RtoC was dramatically reduced to the same level as that of the nonlethal 17X line. (B) Parasitemia of 17X-CtoR was significantly higher than parental 17X and control 17X-CtoC on days 4 and 5 ($P < 0.001$), the acute phase of infection; however, the pattern observed is intermediate between the lethal 17XL and nonlethal 17X lines. Parasitemias are plotted using the geometric mean and SD of log-transformed data from groups of 5 mice. (C) All mice infected with 17XL-RtoC survived, whereas all mice infected with parental 17XL and control 17XL-RtoR lines died by day 7. All mice infected with 17X, 17X-CtoC, and 17X-CtoR survived.

MICROBIOLOGY

determinant of the difference between lethal and nonlethal lines of *P. y. yoelii* parasites. This substitution alters the intracellular organelle localization of *Py*EBL from the micronemes to the dense granules and alters the erythrocyte-type invasion preference, course of infection, and parasite virulence in the host.

The crystal structure of region 6 of *P. falciparum* EBA-175 indicates that the second Cys residue forms a disulfide bridge with the fourth Cys residue in this region. Arg substitution of the second Cys residue in the *P. yoelii* 17XL line abolishes this disulfide bridge and thus likely destroys the region 6 structure, which is critical for the trafficking of the protein to the micronemes. It is possible that an incorrectly folded region 6 would not allow the protein to be properly recognized by an (as yet uncharacterized) partner molecule responsible for the trafficking of the EBL protein to the micronemes (9). The mechanism involved in the trafficking of the mutated protein to the dense granules remains unresolved.

Using genetic modification, we have demonstrated that when *Py*EBL is trafficked to the microneme in the 17XL line genetic background, the erythrocyte-type invasion preference and the course of infection are comparable to those of the nonlethal 17X line. This indicates that the substitution of Cys to Arg is a major determinant of the lethal phenotype of the 17XL line. However, when *Py*EBL was not trafficked to the microneme in parasites with the 17X line genetic background, the course of infection was intermediate between the 2 parental lines, suggesting that although *Py*EBL is a critical determinant, other factor(s) are also involved in the lethal phenotype of the 17XL line. In *P. falciparum*, the expression of EBL seems to be co-operationally regulated with another *Plasmodium* ligand encoded by the *rbl (reticulocyte-binding-like)* multigene family that is composed of 6 members in *P. falciparum* and at least 14 members in *P. yoelii* (14–16); thus, the *P. yoelii rbl* protein, Py235, is a potential candidate for such factor(s). Consistent with this hypothesis is the finding that when Py235 expression was suppressed, the course of infection of the lethal *P. yoelii* YM line was altered from a lethal pattern to an intermediate pattern similar to that observed in the 17X-CtoR line shown in this study (17). On the basis of these observations, we propose that *Py*EBL may preferentially recognize reticulocytes and that the removal of *Py*EBL from the micronemes may result in free space within this organelle that may subsequently be filled with other ligand(s), possibly Py235, which consequently enables the parasite to invade a variety of erythrocyte types. Because different Py235 proteins may have different receptor specificities, parasite invasion preference and the subsequent course of infection may vary, depending on the Py235 member that fills the free space in the micronemes created by the absence of *Py*EBL. Such a switching mechanism for an erythrocyte invasion pathway has been previously proposed for *P. falciparum* (18).

A Linkage Group Selection analysis conducted by Pattaradilokrat et al. (19) identified a chromosomal region that included the *ebl* gene locus as a major determinant in the multiplication rate differences between the lethal *P. y. yoelii* YM line and a nonlethal 33X line, supporting the role of the EBL protein in controlling virulence phenotypes. Consistent with our findings that another genetic factor may be involved, they also identified a further genomic region on *P. yoelii* chromosome 5 or 6 that showed weak association with multiplication rate.

Because *Py*EBL localized in the dense granules is potentially nonfunctional, we attempted to disrupt the *pyebl* gene locus in both the 17X and 17XL lines (Fig. S7). However, repeated attempts failed to achieve this, despite the successful genomic integration of the control plasmid. This indicates that *Py*EBL is essential for parasite survival, even when it is not trafficked to the microneme. Two possible explanations for this may be that (*i*) an undetectable amount of *Py*EBL may still localize in the micronemes and remain functional, or (*ii*) *Py*EBL is

functional during erythrocyte invasion (or for another unknown critical role during the life cycle), even when localized in the dense granules. Although a subgroup of the dense granules, known as exonemes, were recently reported to secrete their contents immediately before schizont rupture (20), we found that *Py*EBL was not detected on the surface of released individual merozoites of 17XL parasites (Fig. S8). Thus, the identity of the *Py*EBL-containing dense granules and the timing of *Py*EBL secretion from them, if at all, in the 17XL line remain undetermined.

In summary, we have found that a single nucleotide substitution altered the intracellular localization of the malaria parasite ligand *Py*EBL, which in turn altered erythrocyte invasion preference, course of infection, and parasite virulence. The virulence-mediating mechanism described in this report furthers our understanding of parasite–host interactions and has important implications for malaria vaccine design, especially those based on *Pv*DBP for *P. vivax* malaria.

Materials and Methods

Rodent Malaria Parasites. *Plasmodium yoelii* 17X, 17XL, and YM lines were maintained in BALB/c mice (Charles River Japan). The *P. yoelii* YM line was a kind gift from David Walliker of Edinburgh University.

DNA and RNA Isolation. Parasite genomic DNA (gDNA) was isolated from parasite-infected mouse blood using DNAzol BD reagent (Invitrogen). Parasite-infected blood was passed through a single CF11 cellulose column to remove leukocytes, and a schizont-enriched fraction was collected by differential centrifugation on a 50% Percoll solution (GE Healthcare). Total RNA was isolated from the schizont-enriched fraction using RNeasy Mini Kit (Qiagen). cDNA was synthesized using Omniscript reverse transcriptase (Qiagen) with random hexamer after DNase treatment.

PCR Amplification and Sequencing of *ebl* Genes. *ebl* genes were PCR-amplified from gDNA using KOD Plus DNA polymerase (Toyobo), with specific primers for each *ebl* gene designed using the *P. yoelii* genome database (The Institute for Genomic Research) and the *P. chabaudi* and *P. berghei* genome databases (The Sanger Centre). *ebl* sequences were determined by direct sequencing using an ABI PRISM 310 genetic analyzer (Applied Biosystems) from PCR-amplified products. Sequences were aligned using CLUSTALW implemented in MacVector (version 9.0; Accelrys).

Southern Blot Analysis. Five micrograms of *P. yoelii* gDNA were digested with EcoRI, EcoRV, ClaI, BanI, and NspI, and with BanI and HpaI with appropriate buffer, overnight. Digested gDNA was subjected to electrophoresis on 0.8% agarose gels, followed by alkaline transfer onto a Hybond-*n* + PVDF membrane (GE Healthcare). Probes were first PCR-amplified with 5′–TAAATCTA-AATGGGATACAT–3′ and 5′–AGTTGGATTGATAGTTACAGATTC–3′ primers for the *pyebl* region, cloned into pGEM-T Easy plasmid (Promega), digested from the plasmid, and then hybridized onto membranes. Probes were labeled with the AlkPhos Direct kit (GE Healthcare), and a chemiluminescent signal developed with CDP-*star* reagent (GE Healthcare) was recorded on RX-U film (Fujifilm).

Recombinant Proteins. Expression plasmids were constructed on the basis of the pEU-E01-G(TEV)-N2 vector (21) by inserting PCR products amplified from *P. yoelii* 17X gDNA using KOD Plus DNA polymerase with the following primers: 5′-gaga<u>CTCGAG</u>GTTAATTTATTAAAAAGAACATATGAATCTTTCC-3′ and 5′-tctc<u>GGATCC</u>**CTA**TGAATAGCTCTCTTTTTGAAAAC-3′ for *Py*EBL regions 1 to 6 (R1–6; amino acid positions 28–787), 5′-gaga<u>CTCGAG</u>GTTAATTTATTA-AAAAGAACATATGAATCTTTCC-3′ and 5′-tctc<u>GGATCC</u>**CTA**CAAATTATTATTA-ATAGGAGTATTACTGGG-3′ for regions 1 to 2 (R1–2; 28–436), 5′-gaga<u>CTC-GAG</u>GAAAAAAATGGAAATGTAAATTACAAAG-3′ and 5′-tctc<u>GGATCC</u>**CTA**-CAAATTATTATTAATAGGAGTATTACTGGG-3′ for region 2 (R2; 113–436), 5′-gaga<u>CTCGAG</u>TCTTCTGTTAAACCCAGTAATAC-3′ and 5′-tctc<u>GGATCC</u>**CTA**T-ACATTTTCGTTGGCTAGC-3′ for regions 3 to 5 (R3–5; 423–716), and 5′-gagagaga<u>CTCGAG</u>GACCCTAAACATGTATGTGTTGATAC-3′ and 5′-gagagaga<u>GGATCC</u>**TCA**TCCCATAAAGCTGGAAGAACTACAG-3′ for the 19-kDa region of the merozoite surface protein 1, *Py*MSP1 (*Py*MSP1–19; 1658–1757). The stop codon is shown in bold letters, and XhoI and BamHI restriction sites are underlined. GST-fused *Py*EBL or *Py*MSP1–19 recombinant proteins were expressed using the wheat germ cell-free protein synthesis system (Protemist DT; CellFree Sciences). Recombinant proteins were captured by a glutathione

column, washed, and eluted with glutathione elution buffer. Protein synthesis was confirmed by SDS-PAGE and Coomassie Brilliant Blue protein staining. Recombinant *Py*EBL R1–6 and R3–5 and *Py*MSP1–19 were used to produce antibodies, and *Py*EBL R1–2 and R2 were used for Western blot analysis.

Antibodies. To produce mouse anti-*Py*EBL and anti-*Py*MSP1 sera, female BALB/c mice were i.p. immunized 5 times with recombinant *Py*EBL R1–6 or 3 times with recombinant *Py*MSP1–19 emulsified with Freund's adjuvant, and killed for serum collection. To produce rabbit anti-*Py*EBL R3–5 serum, a female Japanese white rabbit was s.c. immunized 3 times with recombinant *Py*EBL R3–5 emulsified with Freund's adjuvant. To produce mouse anti-*Py*EBL monoclonal antibodies, the spleen was removed from a mouse immunized with recombinant *Py*EBL R1–6, and spleen cells were fused with a mouse myeloma cell line derived from a BALB/c mouse by the conventional polyethylene glycol method. Supernatants of cultured hybridoma colonies were tested with recombinant *Py*EBL R1–6 by ELISA and on *P. yoelii* 17X blood smears by indirect immunofluorescent assay. Positive hybridoma colonies were selected and cloned by 2 rounds of limiting dilution. The epitope region of each monoclonal antibody was tested by Western blot with a panel of recombinant *Py*EBL proteins. Anti-AMA1 rabbit serum was a gift from Carole Long of the National Institutes of Health.

Immunofluorescence Microscopy. *P. yoelii*–infected mouse erythrocytes were smeared onto glass slides, air dried, and stored at −80 °C without fixation. Slides were thawed, acetone-fixed, preincubated with PBS containing 5% nonfat milk at 37 °C for 30 min, incubated with mouse anti-*Py*EBL and rabbit anti-AMA1 sera at room temperature for 1 h, and then incubated with FITC-conjugated goat anti-(mouse IgG and IgM) antibody (Biosource International) and Alexa-546–conjugated goat antirabbit IgG antibody (Molecular Probes) at 37 °C for 30 min. Parasite nuclei were stained with DAPI. Differential interference contrast (DIC) and fluorescent images were obtained using a fluorescence microscope (BX50; Olympus) with a CCD digital camera (DC500; Leica) and processed using Adobe Photoshop CS (version 8.0; Adobe Systems).

Immunoelectron Microscopy. *P. yoelii*–infected mouse blood was fixed in 1% paraformaldehyde–0.1% glutaraldehyde in Hepes-buffered saline and embedded in LR white resin (Polysciences). Sections were blocked for 30 min in PBS–milk–Tween 20, incubated overnight at 4 °C in PBS–milk–Tween 20 containing mouse anti-*Py*EBL R1–6 serum, and then incubated for 1 h in PBS–milk–Tween 20 containing goat antimouse IgG conjugated with gold particles (10 nm diameter; Jansen). Sections were stained with 2% uranyl acetate in 50% methanol and examined by electron microscopy (JEM-1230; JEOL).

Genetic Modification of the *pyebl* Gene Locus. Two basic plasmids, pPbDT3U-B12 and pHDEF1-mh-R12, were constructed. A DNA fragment encoding cyan fluorescent protein was PCR-amplified from pECFP-C1 plasmid (Stratagene) using KOD Plus DNA polymerase with primers 5′-agcGCTAGCGTGAG-CAAGGGCGAG-3′ (NheI site is underlined) and 5′-gacGTCGACGGATCCTCTA-GACTTGTACAGCTCGTCC-3′ (SalI and XbaI sites are underlined, and BamHI site is shown in bold) and ligated into the pGEM-T Easy plasmid. The insert was then digested with NheI and SalI, purified, and ligated into pRGDT-B12 (22) using the NheI and SalI sites, yielding pRCDT-B12. pRCDT-B12 was digested with ClaI and XbaI and filled with an oligonucleotide linker comprising cgatCTCGAGCCCGGGt and ctagaCCCGGGCTCGAGat to generate XhoI (underlined) and SmaI (bold) sites to yield pPbDT3U-B12. pHDEF1-mh (23) was digested with SmaI and ApaI to remove the 3′ untranslated region of histidine-rich protein 2, the ApaI cohesive end was blunted, and a Gateway gene conversion cassette C1 (Invitrogen) was inserted. The XhoI site was destroyed by XhoI digestion, filled in using KOD Plus DNA polymerase, and self-ligated to yield pHDEF1-mh-R12.

To modify the *pyebl* gene locus, a DNA fragment encoding *Py*EBL region

6 to the stop codon was PCR-amplified from gDNA of the *P. yoelii* 17XL line with primers 5′-gCCATGGGAACATAGAGACATTAAAAAAAGC-3′ and 5′-gCTCGAGATAAAAATCTACAGGTATATATTC-3′ (NcoI and XhoI sites are underlined) and cloned into pGEM-T Easy plasmids. The insert was ligated into the NcoI and XhoI sites of pPbDT3U-B12 to yield pR6Cyt-B12. DNA fragments encoding *Py*EBL region 3 to the stop codon were PCR-amplified from cDNA of the *P. yoelii* 17X and 17XL lines with primers 5′-atCTTCTGTTA-AACCCAGTAATAC-3′ and 5′-ccAGATCTTTAATAAAAATCTACAGG-TATATATTC-3′ (BglII site is underlined). PCR products were then ligated into the SmaI site of pR6Cyt-B12, yielding pR6Cyt+R3Cyt(X)-B12 and pR6Cyt+R3Cyt(XL)-B12, respectively. pR6Cyt+R3Cyt(X)-B12 and pR6Cyt+R3Cyt(XL)-B12 were subjected to a BP recombination reaction with the donor vector pDONR221 (Invitrogen) to produce the corresponding entry plasmids pENT.R6Cyt+R3Cyt(X) and pENT.R6Cyt+R3Cyt(X). These entry plasmids were subjected to a LR recombination reaction (Invitrogen), according to the manufacturer's instructions, with pHDEF-1-mh-R12 to yield replacement constructs pYEBL-R6Cyt+R3Cyt(X) and pYEBL-R6Cyt+R3Cyt(XL), respectively.

P. yoelii schizont-enriched fraction was collected by differential centrifugation on 50% HistoDenz in PBS, and 20 μg of XhoI-digested transfection constructs were electroporated to 5×10^7 of enriched schizonts using the Nucleofector device (Amaxa) with human T cell solution under program U-33 (24). Transfected parasites were i.v. injected into 8-week-old BALB/c female mice, which were treated by i.p. injection with 1 mg/kg of pyrimethamine daily. Before inoculation of 17X line parasites, mice were treated with phenylhydrazine to increase the reticulocyte population in the blood. Drug-resistant parasites were cloned by limiting dilution. Integration of the transfection constructs was confirmed by PCR amplification with a unique set of primers for the modified *pyebl* gene locus, followed by sequencing and Southern blot analysis.

Course of Infection. To assess the course of infection of transgenic and WT parasite lines, 1×10^6 parasitized erythrocytes were injected i.v. into 8-week-old female BALB/c mice. Thin blood smears were made daily, stained with Giemsa's solution, and parasitemias were recorded. Mouse survival was evaluated by the Kaplan-Meier method. Parasitemias of each group were compared by 1-way ANOVA and Tukey's posttest, implemented in Prism 4.0 (GraphPad Software).

Selectivity Index. To compare erythrocyte preference between transgenic and WT *P. yoelii* parasite lines, a SI was calculated as follows: Multiple-infected erythrocytes divided by the expected number of multiple-infected erythrocytes, which was calculated from the number of infected erythrocytes and parasitemia (13). When the preferred erythrocyte type is limited, the observed number of multiple-infected erythrocytes increases. More than 200 parasitized erythrocytes were examined on Giemsa-stained thin blood smears collected on postinoculation day 3. The SI of each group was compared by 1-way ANOVA and Tukey's posttest, implemented in Prism 4.0.

For additional information see *SI Materials and Methods*.

1. Landau I, Gautret P (1998), in *Malaria: Parasite Biology, Pathogenesis, and Protection*, ed Sherman IW (American Society for Microbiology, Washington, DC), pp 401–417.
2. Yoeli M, Hargreaves B, Carter R, Walliker D (1975) Sudden increase in virulence in a strain of *Plasmodium berghei yoelii*. *Ann Trop Med Parasitol* 69:173–178.
3. Playfair JH, De Souza JB, Cottrell BJ (1977) Protection of mice against malaria by a killed vaccine: Differences in effectiveness against *P. yoelii* and *P. berghei*. *Immunology* 33:507–515.
4. Miller LH, Mason SJ, Clyde DF, McGinniss MH (1976) The resistance factor to *Plasmodium vivax* in blacks. The Duffy-blood-group genotype, FyFy. *N Engl J Med* 295:302–304.
5. Wertheimer SP, Barnwell JW (1989) Plasmodium vivax interaction with the human Duffy blood group glycoprotein: Identification of a parasite receptor-like protein. *Exp Parasitol* 69:340–350.
6. Greenwood BM, et al. (2008) Malaria: Progress, perils, and prospects for eradication. *J Clin Invest* 118:1266–1276.
7. Adams JH, et al. (1992) A family of erythrocyte binding proteins of malaria parasites. *Proc Natl Acad Sci USA* 89:7085–7089.
8. Withers-Martinez C, et al. (2008) Malarial EBA-175 region VI crystallographic structure reveals a KIX-like binding interface. *J Mol Biol* 375:773–781.
9. Treeck M, et al. (2006) A conserved region in the EBL proteins is implicated in microneme targeting of the malaria parasite *Plasmodium falciparum*. *J Biol Chem* 281:31995–32003.

Otsuki et al.

10. Sim BK, Toyoshima T, Haynes JD, Aikawa M (1992) Localization of the 175-kilodalton erythrocyte binding antigen in micronemes of *Plasmodium falciparum* merozoites. *Mol Biochem Parasitol* 51:157–159.

11. Adams JH, et al. (1990) The Duffy receptor family of *Plasmodium knowlesi* is located within the micronemes of invasive malaria merozoites. *Cell* 63:141–153.

12. Torii M, Adams JH, Miller LH, Aikawa M (1989) Release of merozoite dense granules during erythrocyte invasion by *Plasmodium knowlesi. Infect Immun* 57:3230–3233.

13. Simpson JA, Silamut K, Chotivanich K, Pukrittayakamee S, White NJ (1999) Red cell selectivity in malaria: A study of multiple-infected erythrocytes. *Trans R Soc Trop Med Hyg* 93:165–168.

14. Stubbs J, et al. (2005) Molecular mechanism for switching of *P. falciparum* invasion pathways into human erythrocytes. *Science* 309:1384–1387.

15. Iyer J, Grüner AC, Rénia L, Snounou G, Preiser PR (2007) Invasion of host cells by malaria parasites: A tale of two protein families. *Mol Microbiol* 65:231–249.

16. Carlton JM, et al. (2002) Genome sequence and comparative analysis of the model rodent malaria parasite *Plasmodium yoelii yoelii. Nature* 419:512–519.

17. Iyer JK, Amaladoss A, Ganesan S, Preiser PR (2007) Variable expression of the 235 kDa rhoptry protein of *Plasmodium yoelii* mediate host cell adaptation and immune evasion. *Mol Microbiol* 65:333–346.

18. Duraisingh MT, Maier AG, Triglia T, Cowman AF (2003) Erythrocyte-binding antigen 175 mediates invasion in *Plasmodium falciparum* utilizing sialic acid-dependent and -independent pathways. *Proc Natl Acad Sci USA* 100:4796–4801.

19. Pattaradilokrat S, Culleton RL, Cheesman SJ, Carter R (2009) Gene encoding erythrocyte binding ligand linked to blood stage multiplication rate phenotype in *Plasmodium yoelii yoelii. Proc Natl Acad Sci USA*, 10.1073/pnas.0811430106.

20. Yeoh S, et al. (2007) Subcellular discharge of a serine protease mediates release of invasive malaria parasites from host erythrocytes. *Cell* 131:1072–1083.

21. Tsuboi T, et al. (2008) Wheat germ cell-free system-based production of malaria proteins for discovery of novel vaccine candidates. *Infect Immun* 76:1702–1708.

22. Ghoneim A, Kaneko O, Tsuboi T, Torii M (2007) The *Plasmodium falciparum* RhopH2 promoter and first 24 amino acids are sufficient to target proteins to the rhoptries. *Parasitol Int* 56:31–43.

23. Fernandez-Becerra C, de Azevedo MF, Yamamoto MM, del Portillo HA (2003) Plasmodium falciparum: New vector with bi-directional promoter activity to stably express transgenes. *Exp Parasitol* 103:88–91.

24. Janse CJ, et al. (2006) High efficiency transfection of *Plasmodium berghei* facilitates novel selection procedures. *Mol Biochem Parasitol* 145:60–70.

Otsuki et al.